

Effect of anisotropy on Brillouin spectra of stripe-structured cobalt layers

S. M. Chérif,* Y. Roussigné, and P. Moch

CNRS, Laboratoire des Propriétés Mécaniques et Thermodynamiques des Matériaux (UPR 9001), Université Paris-Nord, 93430 Villetaneuse, France

(Received 17 March 1998; revised manuscript received 25 September 1998)

We present a comparative study of the magnetic Brillouin spectra of arrays of stripe-structured Co layers and of continuous unpatterned Co films. These spectra mainly differ from each other through the occurrence of an additional line on the low-frequency side for the patterned films. This feature is related to magnetic eigenmodes arising from the uniform bulk mode of the continuous film when taking into account the magnetic anisotropy in the dipolar approximation: the simultaneous presence of magnetic anisotropy and of structuration is needed to allow for light scattering by such pseudobulk modes. In the case of continuous films the spectral profiles that contain lines related to both the Damon-Eshbach and to standing spin waves are quantitatively interpreted. An approach to the magnetic eigenmodes observed in the stripes is developed; it is derived from a calculation that uses the dipolar approximation and includes anisotropy for cylinders with elliptical cross section. Finally, the influence of the demagnetizing field upon the spectra of the patterned layers is evidenced and discussed. [S0163-1829(99)12013-7]

I. INTRODUCTION

The magnetic properties of layered systems differ significantly from those of their bulk analogs,¹ a phenomenon which is widely attributed to dimensional reduction. Many papers on spin waves in continuous films have already contributed to a better understanding of such magnetic excitations; much less is known however about thin films patterned into stripes or dots.²⁻⁵

Brillouin light scattering, which allows access to the electromagnetic radiation inelastically scattered by the thermal spin waves, provides a powerful nondestructive tool in the investigation of the parameters monitoring the physical properties of magnetic thin films. The steadily growing applications in magnetic recording media technology like storage devices and sensors technologies^{6,7} partly motivate the interest in the determination of those parameters. The magnetic properties of such artificial structures are however expected to be very different from those of a two-dimensional ferromagnetic layer, because of their reduced size, specific shape, and of periodic structure of the studied arrays.

The theoretical determination of magnetostatic spin waves modes with small but finite wave vector \mathbf{q} in a single ferromagnetic slab was performed by Damon and Eshbach (DE).⁸ In the DE calculation, the dipolar approximation was used and the magnetic anisotropy was neglected. Further calculations were performed by many authors,⁹⁻¹² so as to include the magnetic exchange, the volume as well as surface anisotropy, and dissipative effects. In flat unbounded films various modes are expected to propagate with wave vectors in the plane of the film. Schematically, for the direction of magnetization aligned perpendicular to the in-plane wave vector \mathbf{q}_{\parallel} , the theory yields two types of spin-wave modes: (i) one nonreciprocal surface wave for in-plane propagation, so-called Damon-Eshbach mode, which consists of a dipolar-dominated wave, and (ii) the bulk spin waves which are excitations of the whole magnetic system [often called standing spin waves (SSW)] and are exchange-dominated modes. If

anisotropy and exchange are neglected, an analytical expression of the frequency of the DE modes is easily obtained. In the presence of anisotropy, the frequencies generally have to be computed numerically,^{13,14} with the exception of ultrathin single magnetic layers which satisfy $q_{\parallel}d \ll 1$ (where d is the thickness) for which analytic expressions of the spin-wave frequencies can be derived.¹⁵ The main effect of the magnetic exchange is to split the bulk modes and to shift them up to higher frequencies; but the exchange can also significantly modify the frequency of the DE mode. The anisotropy mainly acts upon the DE mode but it also affects the SSW mode. All of those can be observed on the Brillouin-scattering spectra; the scattered intensity is related to the magneto-optical modulation of the illuminating light by the oscillating magnetic moment of the spin waves: complete calculations of the spectral shapes have been performed and have proved to satisfactorily fit the experimental data.¹³ Indeed, the selection rules specify that the difference between the tangential component of the wave vectors of the scattered and of the incident light is either the opposite of or equal to the wave vector \mathbf{q}_{\parallel} of the involved spin wave (Stokes spectrum versus anti-Stokes spectrum).

High-frequency dynamic properties of structured magnetic films have been the object of very few studies, all of them concerning Permalloy stripes or Permalloy dots.²⁻⁵ Finite-size effects in the spin-wave spectra of stripes were reported by Gurney *et al.*:² if the spin-wave momentum is laterally confined by the width of the stripe, the DE peak is replaced by a series of modes (stripe modes), the peak intensities of which lay below a Gaussian-like envelope centered at the frequency of the DE mode of the corresponding continuous film. The stripe modes have been interpreted as resonant excitations of dipole-exchange spin-wave normal modes of the narrow stripes. Other finite-size effects related to a possible quantization of the in-plane wave vector have been recently reported on Permalloy dots.⁴ Permalloy has attracted interest because of its very small magnetic anisotropy which, in most cases, can be neglected. De Wames and Wolfram¹⁶

have derived an expression describing the spin-wave modes in an axially magnetized cylinder using the dipolar approximation in the absence of anisotropy and of exchange: they find a series of surface modes that are indexed by the number n of nodes in the angular dependence of the magnetic potential, which roughly corresponds to a quantization along the perimeter of the stripe. They have also shown that the surface mode frequencies are closely related to those obtained by Damon and Eshbach for an infinite film.

In this paper, we present a comparative study of the magnetic Brillouin spectra of arrays of stripe-structured Co layers and of continuous unpatterned Co films. A calculation including anisotropy is performed using the dipolar approximation, which means that the magnetic dipole coupling is large in comparison with the exchange coupling. An implicit expression for the spin-wave frequencies in the case of stripes showing an elliptical cross section is derived. We also comment on the influence of the demagnetizing field arising from the finite width of the stripes. The agreement with our experimental data is discussed.

II. EXPERIMENT

In order to minimize the fluctuations of the parameters related to the elaboration process, all the Brillouin experiments were performed on the same $5 \times 5 \text{ mm}^2$ sample consisting of a Si(111)/SiO₂/Cr(10 Å)/Au(250 Å)/Co(400 Å)/Au(30 Å) sandwich with various patterned or unpatterned zones. The initial unpatterned sandwich was obtained by evaporation: part of it was used to measure the magnetization via the vibrating sample magnetometer (VSM) method. We manufactured $0.75 \times 0.75 \text{ mm}^2$ patterned areas using electron-beam lithography and ion-beam sputtering: micron size periodic arrays of cobalt stripes were etched with width/period ratios of 0.5/1, 0.7/2, 1/1.5, and 2/3 μm , respectively. The remaining parts of the sample were left unpatterned for further comparison of the Brillouin spectra. The fabrication process has been detailed elsewhere¹⁷ and it consists in two steps: (i) fabrication of a resist mask by electron irradiation in a scanning electron microscope (SEM) and selective dissolution of the unprotected areas; (ii) sputtering of the unprotected areas by Ar⁺ ion bombardment in ultrahigh vacuum and further dissolution of the remaining resist. As an illustration of the good definition and of the dimensional control of our fabrication process, Fig. 1 shows a scanning electron micrograph of the array of Co stripes with a 2 μm period and a 0.7 μm width. The Brillouin magnetic backscattered spectra were studied with the help of a 2 \times 3 pass tandem Fabry-Pérot interferometer illuminated by an Ar⁺ ion laser at the wavelength 5145 Å with an incident power of 200 mW; the in-plane momentum transfer \mathbf{q}_{\parallel} was chosen perpendicular to the applied field \mathbf{H} . The spectra were achieved using crossed polarizations between the incident and the scattered beams, in order to prevent the appearance of phonon lines; they were recorded with large accumulation times (2 or 3 h).

III. RESULTS AND DISCUSSION

A. Continuous thin film

Let us first comment upon the results related to the unpatterned area. Figure 2 shows an experimental Brillouin spec-

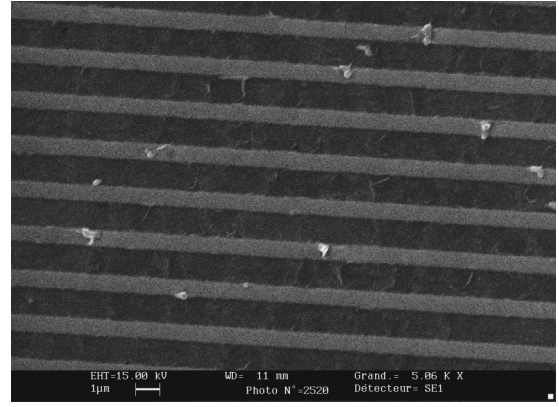


FIG. 1. SEM micrograph of the array of 0.7 μm width–2 μm period cobalt stripes.

trum (a) and a calculated one (b): they were obtained with $H = 2 \text{ kOe}$, using an angle of incidence $\theta_i = 45^\circ$, which leads to an in-plane wave vector $q_{\parallel} = 1.73 \times 10^5 \text{ cm}^{-1}$. Notice the large asymmetry of the Stokes/anti-Stokes spectrum which affects two lines: we checked that the asymmetry is reversed when the sense of \mathbf{H} is reversed, as it should be.

The DE Brillouin line related to the DE mode is present in both the Stokes and the anti-Stokes sides of the spectra, but with a remarkable asymmetry of the intensity: this is caused by the contribution of off-diagonal spin-spin correlation functions to the intensity of the light scattering, while the thermal population factor, the localization of the modes, and the characteristics of the magneto-optic tensor do not play a significant role in determining the Stokes/anti-Stokes asymmetry.¹⁸ The first and the second standing spin waves (SSW's) are also observed: the above-mentioned important asymmetry in the intensities of the first standing mode, which is comparable to the asymmetry found for the DE lines, is in agreement with our numerical calculation. The method of calculation of the spectrum, which is based on the

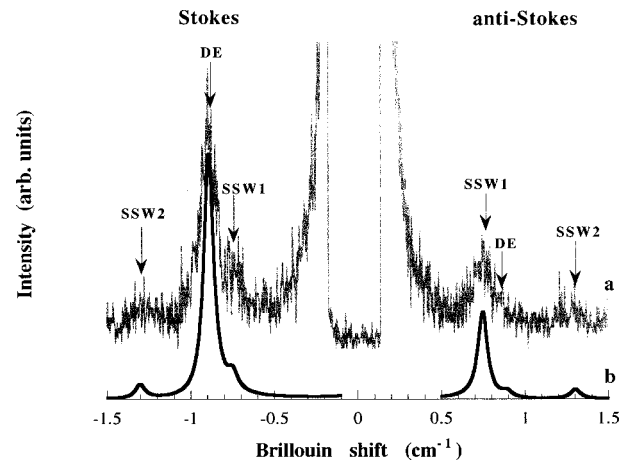


FIG. 2. Brillouin spectra of the unpatterned cobalt layer: (a) experimental, (b) calculated. Backscattering with $\theta_i = 45^\circ$, $H = 2 \text{ kOe}$. The calculated spectrum is provided with $H_a = 2.6 \text{ kOe}$. In this figure and in the following ones the values of $4\pi M$, of γ and of the magnetic exchange are taken from the published ones in bulk Co ($4\pi M = 17.6 \text{ kOe}$, $\gamma = 1.9 \times 10^7 \text{ Hz/Oe}$, i.e., $g = 2.16$, $D = 2.6 \times 10^{-9} \text{ Oe/cm}^{-2}$).

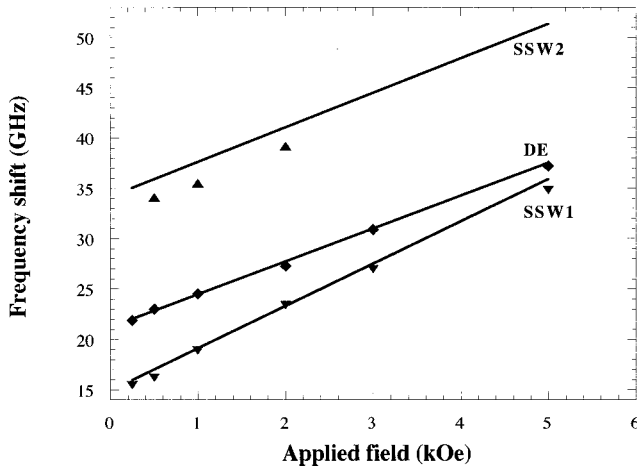


FIG. 3. Variations of the frequencies of the DE, SSW1, and SSW2 lines of the unpatterned area versus the applied magnetic field for $\theta_i=45^\circ$. The symbols represent the experimental values. The full lines are the calculated ones using: $4\pi M=17.6$ kOe, $\gamma=1.9\times 10^7$ Hz/Oe, i.e., $g=2.16$, $D=2.6\times 10^{-9}$ Oe/cm $^{-2}$, $H_a=2.6$ kOe.

evaluation of the appropriate spin-dependent response functions (Green functions) has been reported elsewhere.¹³ Due to the strong coupling between the DE and the first standing mode (SSW1), the usual approximate expressions for their frequencies lead to rather large errors and our method was found necessary not only, as is usually the case, so to provide a correct evaluation of the shapes of the spectra, but also so as to account for the positions of the maxima which do in practice coincide with the frequencies of the studied surface modes. The agreement between the experimental spectrum and the calculated one is very satisfactory: it was obtained by fitting the anisotropy field H_a (assumed to be uniaxial) using the published values of the magnetization ($4\pi M=17.6$ kOe), of the gyromagnetic factor ($\gamma=1.9\times 10^7$ Hz/Oe, i.e., $g=2.16$) and of the magnetic exchange ($D=2.6\times 10^{-9}$ Oe/cm $^{-2}$) in bulk cobalt: except in the case of ultrathin samples where these parameters can suffer substantial modifications, such assumptions were found to be correct in the case of Co layers, from the standpoint of both experimental results¹⁹ and theoretical expectations.²⁰ In contrast, the reported values of the anisotropy field, which, for the Co thickness of our sample, mainly derives from the volume energy density of anisotropy, show a large dispersion: in previous studies concerning Co films grown on a Au sublayer,¹³ we measured values varying from 1 to 4.5 kOe. With these conditions, we find $H_a=2.6$ kOe. The fits remain satisfactory when varying the applied magnetic field H so as to sweep the ~ 0.25 –5 kOe investigated interval as shown in Fig. 3. This figure compares the experimental values for the DE, the SSW1 and the SSW2 frequencies with the expected ones, using the above-mentioned values of the magnetic parameters: the agreement is excellent for the DE line (mean-square deviation of 0.25 GHz) and satisfactory for the SSW1 line (mean-square deviation of 0.6 GHz); the larger value obtained in the case of the SSW1 mode is related to experimental uncertainties due to the weaker intensity and to the wider breadth; the SSW2 line is, in most cases, very weak and hardly observable, which explains a poorer agreement. It is also possible to simultaneously derive $4\pi M$ and H_a from

the analysis of both DE and SSW lines frequencies. With such a protocol, we find $4\pi M=(17.5\pm 1)$ kOe and $H_a=(2.5\pm 1)$ kOe. On the other hand, we have evaluated $4\pi M$ by direct magnetic measurements using the VSM method: the bulk value of $4\pi M$ provides a Co thickness of 420 Å with a precision of about 2%; since the initial precision on the evaluation of the thickness through a quartz balance does not exceed 5%, the above assumption upon $4\pi M$ is perfectly coherent. In view of these results, considering that, in our study, the most precise measurements concern the DE line and that we are interested in the variation of the anisotropy field, if any, but not its absolute value, we postulated that the magnetization does not differ from its bulk value and only used the DE line behavior to fit the subsequent spectra. But, one should not completely disregard the occurrence of a small deviation of the magnetization from the measured value in bulk Co: numerical calculations show that, for small variations of the magnetization, a satisfactory fit can be obtained by varying H_a in order to maintain $(4\pi M-H_a)$ approximately constant. In the remainder of the paper the above-mentioned 2.6 kOe value of the anisotropy field in the unpatterned area has to be considered as a relative reference and we strive to detect its possible variations on the patterned area. Finally, for the studied samples, the DE modes frequencies significantly depend upon the magnetic exchange interaction: as a consequence, any attempt to fit the anisotropy field using the dipolar approximation for the frequency calculation of such pseudo-DE modes leads to an underestimation of H_a . This will complicate the following discussion concerning the patterned structures.

B. Stripe-structured arrays

Figure 4 shows the Brillouin spectra arising from both the continuous unpatterned area (a) and the various stripe-structured areas [(b), (c), (d), (e)] obtained with the following experimental conditions: $H=3$ kOe; $\theta_i=45^\circ$; in the case of the patterned arrays, the magnetic field is applied along the axis of the stripes so as to cancel the demagnetizing field. Surprisingly, in addition to the Brillouin lines already observed and commented upon (DE and SSW), this latter spectrum displays a lower frequency structure, pseudobulk mode (PBM) on both Stokes and anti-Stokes sides with intensities which are far from being negligible. The Stokes/anti-Stokes intensity ratio does not markedly differ from those observed for the DE and the first standing spin waves lines.

This low-frequency line, which is present for all the Co stripe arrays, shows a significantly reduced relative intensity in the widest stripe [(e), 2 μm width]. Up to now such a low-frequency feature has not been reported in any Brillouin study concerning patterned films (stripes or dots): but, as mentioned above, all these previous measurements concern Permalloy which, as is well known, shows very weak magnetic anisotropy. On the other hand, such a low-frequency mode is also absent in unpatterned layers with a strong magnetic anisotropy (e.g., Co films¹³), for which the experimental shape of the spectra agrees well with that numerically predicted:¹³ in the latter case, there are still low eigenfrequency solutions of the equations of motion, apparently related to modes issued from the well-known uniform bulk mode in vanishing anisotropy, *but* these low-frequency

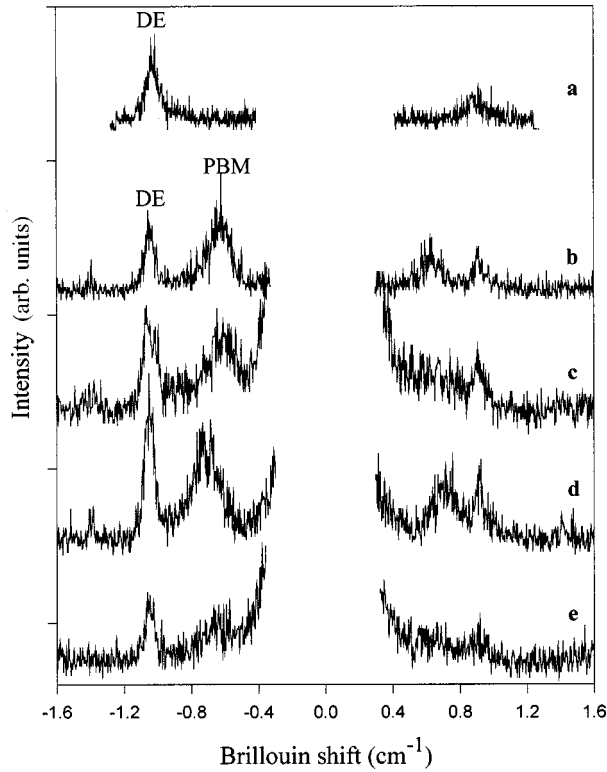


FIG. 4. Experimental Brillouin spectra obtained from both the unpatterned area (a) and various width/period ratios patterned areas: (b) 0.7/2 μm ; (c) 0.5/1 μm ; (d) 1/1.5 μm ; (e) 2/3 μm using the following experimental conditions: $\theta_i = 45^\circ$, $H = 3$ kOe; magnetic field applied parallel to the axis of the stripes for the patterned area.

modes do not contribute to the Brillouin scattering, as experimentally found and theoretically computed with the help of appropriate correlation functions which monitor the scattered intensity.¹³ We then suggest that anisotropy and patterned structuration are necessary ingredients in order to produce a measurable Brillouin intensity of this low-frequency spectrum and that they have to be simultaneously present in

the studied samples. Consequently, as a first step in view of a future complete quantitative understanding of the observed spectra, we present below a calculation of the eigenmodes for magnetic cylindrical stripes showing uniaxial anisotropy with an elliptical cross section. A calculation neglecting the anisotropy has been previously performed by De Wames and Wolfram, in the dipolar approximation.¹⁶ They found the following relation:

$$\left(\frac{\omega}{\gamma}\right)^2 = (H + 2\pi M)^2 - (2\pi M)^2 \left(\frac{a-b}{a+b}\right)^{2n}, \quad (1)$$

where ω is the angular frequency, γ is the gyromagnetic factor, $4\pi M$ is the saturation magnetization; a and b are the parameters of the elliptical cross section and are, respectively, related to the width (x direction) and thickness (y direction) of the stripe. n is an integer which can be taken non-negative. Notice that for $n=0$, expression (1) provides the frequency of the uniform dispersionless bulk mode: $\gamma[H(H + 4\pi M)]^{1/2}$. For $b/a \ll 1$, it can be easily shown that expression (1) is equivalent to the well-known relation in the dipolar approximation⁸ for the Damon-Eshbach propagating mode in an infinite layer with an in-plane wave vector \mathbf{q}_{\parallel} , assuming that $q_{\parallel} = n/a$ (as pointed out by De Wames and Wolfram¹⁶): it differs from the naive correspondence ($q_{\parallel} = \pi n/2a$) that one would intuitively derive by assuming that the perimeter of the cross section ($\cong 4a$) is equal to the product of the wavelength by an integer. Such a simple argument is only valid when the penetration depth ($\cong 1/q_{\parallel} = a/n$) of the DE mode is negligible compared to the thickness $2b$, i.e., when $2nb/a$ is significantly larger than 1. Notice that, for Brillouin backscattering studies in infinite layers, q_{\parallel} has to be equated to $(4\pi/\lambda)\sin(\theta_i)$, where λ is the wavelength of the illuminating beam and θ_i is the angle of incidence: numerically, for $a = 3.5 \times 10^{-7}$ m and $\theta_i = \pi/4$, one finds $n=6$ and $2nb/a = 0.7$, which does not satisfy the condition $2nb/a \gg 1$.

We have generalized the above calculation to nonzero uniaxial anisotropy, thus deriving the following expression (see the Appendix):

$$\left(\frac{la-b}{la+b}\right)^{2n} = \frac{(4\pi M\Omega)^2 - \{[H(H-H_a) - \Omega^2](1+l) + 4\pi Ml(H-H_a)\}^2}{(4\pi M\Omega)^2 - \{[H(H-H_a) - \Omega^2](1-l) - 4\pi Ml(H-H_a)\}^2}, \quad (2)$$

where $\Omega = \omega/\gamma$; $H_a = 2K/M$ is the anisotropy field corresponding to uniaxial anisotropy energy equal to $-K(M_y^2/M^2)$; l is given by the relation

$$l^2 = \frac{(4\pi M + H - H_a)H - \Omega^2}{(4\pi M + H)(H - H_a) - \Omega^2}. \quad (3)$$

If the anisotropy vanishes, l is equal to 1, and then relation (2) is equivalent to relation (1). Here again, assuming $b/a \ll 1$, it is easily proved (see the Appendix) that the solu-

tions tend to the obtained ones for modes propagating in an infinite thin film of thickness $2b$ with a wave vector \mathbf{q}_{\parallel} such as $q_{\parallel}a = n$.

Coming back to expression (2) one can distinguish between two cases:

(1) $l^2 > 0$; l is real. In this case, for any given n , expression (2) leads to only one frequency corresponding to the so-called Damon-Eshbach (DE) surface mode in infinite layers.

(2) $l^2 \leq 0$; l is imaginary or vanishes. In this case, expression (2) can lead to several frequencies. If one defines

$$\arg\{(4\pi M\Omega)^2 - [(H(H-H_a) - \Omega^2)(1 - i|l|) - 4\pi Mi|l|(H-H_a)]\} = \alpha(\omega),$$

$$\arg(b + i|l|a) = \beta(\omega).$$

The relation (2) becomes

$$\exp(-4ni\beta(\omega)) = \exp(-2i\alpha(\omega)),$$

i.e.,

$$4n\beta(\omega) = 2\alpha(\omega) + 2(n-p)\pi,$$

where p is an integer.

The frequencies have to be calculated numerically, due to the lack of analytical expressions. One finds that the $l^2 > 0$ solution has to be related to the DE propagating mode in the thin film (still assuming $q_{\parallel} = n/a$ in the limit where $b/a \ll 1$). From Fig. 5, drawn for $n=10$ and for a given set of magnetic parameters, one can derive $(n+1)$ solutions with $l^2 \leq 0$. The frequency difference between two successive $l^2 \leq 0$ [i.e., corresponding to p and $(p+1)$ at constant n] solutions decreases when p increases. At constant p , the frequency dependence upon n is a decreasing function of the anisotropy (Fig. 6). At constant n , the frequency interval swept by the modes related to $l^2 \leq 0$ decreases when the anisotropy field decreases as shown in Fig. 7: it tends to 0 when H_a vanishes and the resulting common frequency takes the value of the above-mentioned uniform bulk mode frequency. When the anisotropy increases the frequency difference between two adjacent $l^2 > 0$ solutions [i.e., corresponding to n and $(n+1)$] decreases (Fig. 8). Finally, one notices that, for reasonable values of the magnetic parameters involved in the model, the frequency differences between the $l^2 \leq 0$ solutions, called pseudobulk modes (PBM's) in all that follows, related to a given value of n are rather small (except, in some cases, for $p=0$, which is not always an available mode as can be seen in Figs. 5 and 10); thus, they are not expected to give rise to a manifold of lines easy to separate in a Brillouin spectrum.

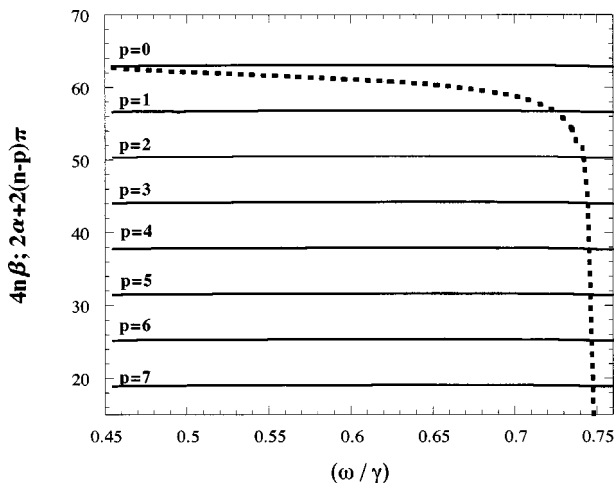


FIG. 5. $[4n\beta(\omega); 2\alpha(\omega) + 2(n-p)\pi]$ versus ω/γ using the conditions: $H=3$ kOe, $H_a=2$ kOe, width $=1$ μm , thickness $=0.05$ μm , $n=10$ (see text). The crossings give the frequencies of the pseudobulk modes.

The above considerations allow at least for a semiquantitative interpretation of the observed spectra in the patterned films. First, we obtain a very good fit of the DE spectrum for $H_a=1.6$ kOe, using $n=6$: the contribution of the mode corresponding to $n=6$ is expected to be the most efficient in the Brillouin-scattering process since it nearly exactly corresponds to the condition $q_{\parallel}a=n$ ($q_{\parallel}=17.3$ μm^{-1} , $a=0.35$ μm), where q_{\parallel} is the wave vector of the involved spin wave when ignoring the influence of the finite width of the stripes. At this stage it is also interesting to notice that the ratio of the thickness to the width is small enough (about 0.06) to provide equivalent values of the frequencies, within the range of the experimental uncertainty, using the approximation of an infinite layer of thickness $2b$ or of an elliptical cylindrical stripe assuming $n=q_{\parallel}a$. The absolute difference is of about 0.4 GHz. The anisotropy field derived from this fit is significantly smaller than that of the unpatterned film (2.6 kOe) but the comparison is difficult since we have neglected the exchange interaction in the case of the patterned structure while exchange was taken into account for the unpatterned sample. To improve the comparison, it is interesting to fit the DE frequency of the infinite thin film in the dipolar approximation: one then finds a reduced value of H_a , as pointed out above; specifically, we obtain $H_a=2$ kOe, to be compared to 1.6 kOe for the patterned structure: the 0.4 kOe gap may result from the elaboration process of the stripes. However, in the absence of a precise calculation of the Brillouin intensity for the patterned structure, one cannot completely exclude that the most efficient mode corresponds to a different value of n ; in this case, the best fit would provide a different anisotropy field. To keep $H_a=2$ kOe, one has to assume $n=8$. Experimental results on Permalloy patterned structures,² have shown that several pseudo-Damon-Eshbach modes simultaneously participate to the scattering, giving rise, in the case of stripes, to separately resolved lines; we believe that in Co stripes the higher anisotropy prevents us from observing such a separation.

We have also studied the Brillouin spectra with an applied magnetic field still in the plane of the stripes but perpendicu-

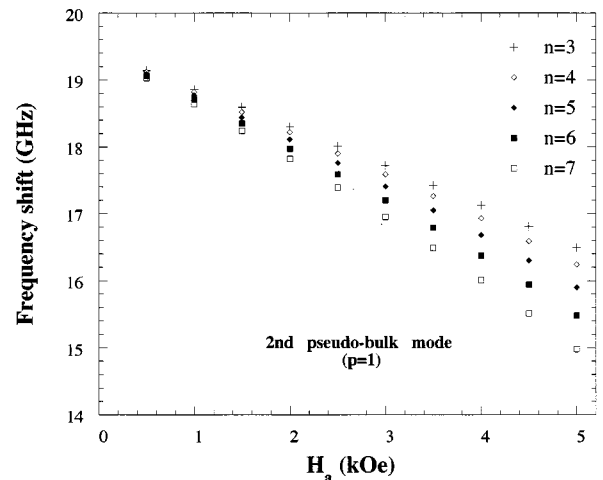


FIG. 6. Frequency shift of the second pseudobulk mode ($p=1$) versus the amplitude of the anisotropy field. The anisotropy favors the separation of modes with adjacent values of n .

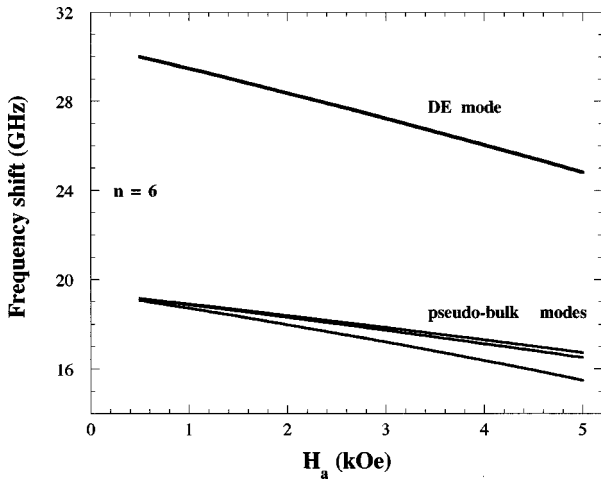


FIG. 7. Frequency shifts of the DE mode and of the pseudobulk modes as a function of the amplitude of the anisotropy field with the conditions: $H = 2$ kOe, $\theta_i = 45^\circ$, i.e., $n = 6$; width = $0.7 \mu\text{m}$; thickness = $0.04 \mu\text{m}$. The anisotropy splits the pseudobulk modes.

lar to their axis. In this case, one has to deal with a demagnetizing field perpendicular to the stripes. On the other hand, with our experimental geometrical arrangement, the observed magnetic modes propagate along the stripes with the wave vector $q_{\parallel} = 17.3 \mu\text{m}^{-1}$. Up to now the evaluations of the frequencies and, moreover, of the Brillouin intensities are still lacking. Experimentally, however, the observed changes in the spectra, compared to the case where the field is parallel to the stripes, mainly arise from the presence of the demagnetizing field. In Fig. 9, the variations of the measured frequencies of the DE lines versus the applied magnetic field have been reported for the parallel and perpendicular directions in the 0.7/2 sample: this last graph is found to be horizontally translated by about 0.65 kOe. We have calculated the mean value of the demagnetizing field over the volume of a stripe, assuming that the magnetization is uniform and perpendicular to its axis and taking into account the interactions between the stripes: in the case of the 0.7/2 samples, we find a value of 1.3 kOe, which is larger than the observed

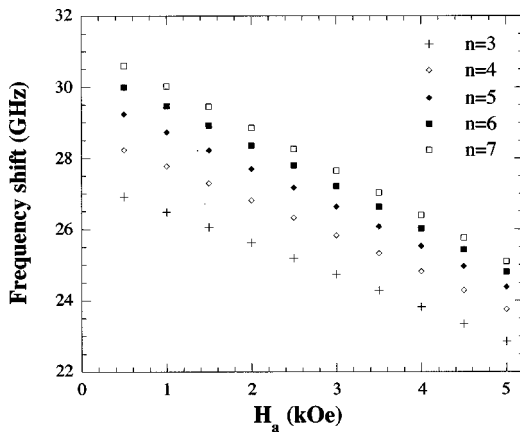


FIG. 8. Frequency shift of the Damon-Eshbach (DE) eigenmode as a function of the amplitude of the anisotropy field with the conditions: $H = 2$ kOe, width = $0.7 \mu\text{m}$, thickness = $0.04 \mu\text{m}$. The anisotropy prevents the separation of modes corresponding to different values of the integer n .

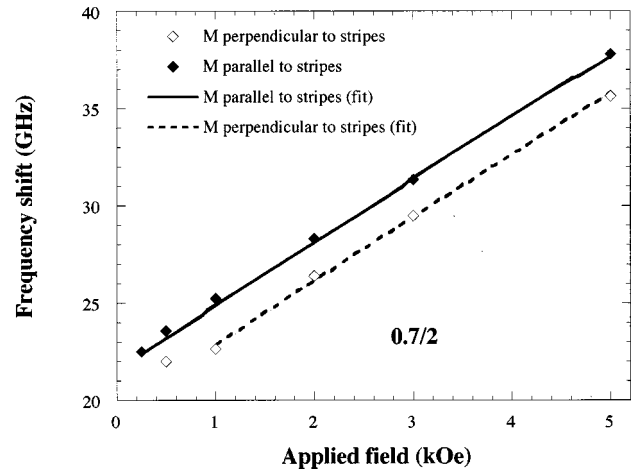


FIG. 9. Variation of the frequency shift of the Damon-Eshbach lines (see Fig. 3) as a function of the applied magnetic field in the 0.7/2 sample for \mathbf{H} parallel and for \mathbf{H} perpendicular to the stripes. The full line is the fit obtained with $H_a = 1.6$ kOe using expression (2) (see text).

0.65 kOe shift but keeps the same order of magnitude. It is worth noticing that the demagnetizing field is far from being uniform in the stripes: in the 0.7/2 structure, for instance, it does not exceed 0.6 kOe at the center of a stripe, to compare to the 1.3 kOe mean value. Qualitatively, we then conclude that the main effects of the variation of the orientation of the applied field arise from the changes of the demagnetizing field but experimental and theoretical further investigations are still needed in order to provide a completely quantitative interpretation.

Finally, in our opinion the major result consists in the observation of the low-frequency spectrum related to the pseudobulk modes. Expression (3) allows us to define a field-dependent frequency interval where $l^2 \leq 0$ modes can be observed, as shown in Fig. 10 (for $H_a = 1.6$ kOe, those are

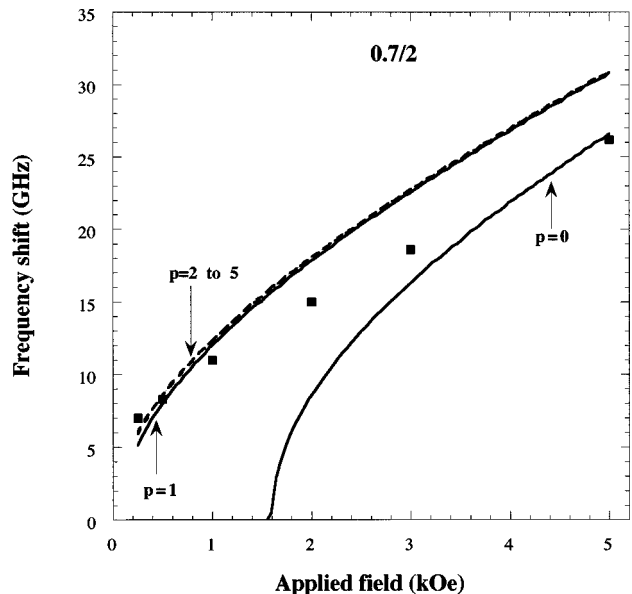


FIG. 10. Variation of the frequency shift of the additional structure (see Fig. 3) as a function of the applied magnetic field. The lines are the boundaries limiting the domain $l^2 < 0$.

derived from the above best fit of the DE mode): the low-frequency observed lines belong to this interval. There are strong arguments to state that these features can be observed only for patterned structures showing large enough magnetic anisotropy, but, here again, in the absence of intensity calculations, more quantitative conclusions would be hazardous.

IV. CONCLUSION

With the help of a previously described lithographic process, we have obtained submicron-size periodic arrays of cobalt stripes and, using Brillouin spectroscopy, have compared their magnetic properties to those of the continuous thin film in which they were prepared. The Brillouin magnetic spectra show an additional structure in the stripe-patterned arrays, absent in the continuous unpatterned layer. In order to interpret the results we have theoretically studied, in the dipolar approximation, various magnetic modes appearing in neighboring geometries consisting into magnetic stripes with an elliptical cross section: our model explicitly takes into account uniaxial anisotropy along one axis of this cross section and we find an implicit expression for the frequencies which generalizes previously published results neglecting the anisotropy; in addition to known features, it gives rise to a set of low-frequency modes originating from the bulk mode existing in the continuous film. The low-frequency spectrum observed in the patterned area is then attributed to these last eigenmodes: experimentally they are Brillouin active only when anisotropy and geometrical patterning are simultaneously present in the studied sample. A complete theoretical analysis of the intensity of the spectra of the patterned areas is still lacking, in contrast with the case of the continuous film where we successfully performed this analysis. However, we could qualitatively explain the differences between the observed spectra of Co and of Permalloy² stripes by the influence of anisotropy which is negligible in the case of Permalloy. Finally, in the case of our studied arrays of Co stripes we have shown the effect of the demagnetizing field.

ACKNOWLEDGMENTS

The authors would like to thank Dr. H. Niedoba for providing us with the cobalt film used in this work and for proceeding to magnetic measurements by VSM, Professor J-F. Hennequin and Professor M. Labrune for fruitful discussions about the manuscript, and Dr. C. Dugautier for his help with the Brillouin measurements.

APPENDIX

In the following formulation, exchange is not included in the equations of motion of the magnetization; hence the modes are due to purely magnetostatic forces (dipolar approximation). We also assume that the distribution of the magnetization in the magnetic stripes satisfies Maxwell equations in the magnetostatic approximation.

The usual approach, which is applied for the calculations, consists of deriving the simultaneous solution of the linearized equation of motion and of the Maxwell's equations with the appropriate electromagnetic boundary conditions.

The Landau-Lifshitz equation is written as

$$\frac{d(\mathbf{M}+\mathbf{m})}{dt} = -\gamma(\mathbf{M}+\mathbf{m}) \times (\mathbf{H}+\mathbf{h}+\mathbf{H}_a+\mathbf{h}_a), \quad (\text{A1})$$

where the uppercase letters refer to the static part and the lowercase letters refer to the dynamic part of the magnetic variables. Assuming a uniaxial anisotropy (density of anisotropy energy: $-K(M_y^2/M^2) = -(H_a/2M)M_y^2$ where H_a defines the usual anisotropy field), it results, after linearization, for oscillations at the frequency $\omega (= \gamma\Omega)$:

$$Hm_x + i\Omega m_y = M \frac{\partial \phi}{\partial x}, \quad (\text{A2})$$

$$-i\Omega m_x + H_b m_y = M \frac{\partial \phi}{\partial y}, \quad (\text{A3})$$

where $H_b = (H - H_a)$, m_x and m_y are the components of the dynamic magnetization, and $\mathbf{h} = \nabla \phi$, where ϕ is the potential related to the demagnetizing field associated to this magnetization.

Using the Maxwell equation

$$\nabla \cdot (\mathbf{h} + 4\pi\mathbf{M}) = 0,$$

we obtain the relation

$$4\pi \frac{\partial m_x}{\partial x} + 4\pi \frac{\partial m_y}{\partial y} + \frac{\partial^2 \phi}{\partial x^2} + \frac{\partial^2 \phi}{\partial y^2} = 0. \quad (\text{A4})$$

From Eqs. (A2), (A3), and (A4),

$$\begin{aligned} & [(4\pi M + H)H_b - \Omega^2] \frac{\partial^2 \phi}{\partial x^2} + [(4\pi M + H_b)H - \Omega^2] \frac{\partial^2 \phi}{\partial y^2} \\ & = 0, \end{aligned} \quad (\text{A5})$$

i.e.,

$$\frac{\partial^2 \phi}{\partial x^2} + l^2 \frac{\partial^2 \phi}{\partial y^2} = 0$$

leading to

$$\phi = f(lx + iy) + g(lx - iy). \quad (\text{A6})$$

Outside the magnetic material, the potential (here labeled ψ) is the solution of

$$\frac{\partial^2 \psi}{\partial x^2} + \frac{\partial^2 \psi}{\partial y^2} = 0 \quad (\text{A7})$$

leading to

$$\psi = \tilde{f}(x + iy) + \tilde{g}(x - iy). \quad (\text{A8})$$

Using a variable u to parametrize the equation of the curve defining the cross section of the magnetic cylinder $[x(u), y(u)]$, the boundary conditions [continuity of the tangential and of the normal components of \mathbf{h} and $(\mathbf{h} + 4\pi\mathbf{M})$, respectively], provide

$$-y'(u) \left(4\pi m_x + \frac{\partial \phi}{\partial x} \right)_{[x(u),y(u)]} + x'(u) \left(4\pi m_y + \frac{\partial \phi}{\partial y} \right)_{[x(u),y(u)]} = -y'(u) \left(\frac{\partial \psi}{\partial x} \right)_{[x(u),y(u)]} + x'(u) \left(\frac{\partial \psi}{\partial y} \right)_{[x(u),y(u)]}, \quad (\text{A9})$$

$$x'(u) \left(\frac{\partial \phi}{\partial x} \right)_{[x(u),y(u)]} + y'(u) \left(\frac{\partial \phi}{\partial y} \right)_{[x(u),y(u)]} = x'(u) \left(\frac{\partial \psi}{\partial x} \right)_{[x(u),y(u)]} + y'(u) \left(\frac{\partial \psi}{\partial y} \right)_{[x(u),y(u)]}. \quad (\text{A10})$$

Using Eqs. (A6) and (A7), we transform Eqs. (A9) and (A10) in

$$\begin{aligned} & \frac{d}{du} \{ [(H_b(H+4\pi M) - \Omega^2)l + 4\pi M\Omega]f - [(H_b(H+4\pi M) - \Omega^2)l - 4\pi M\Omega]g \}_{[x(u),y(u)]} \\ & = (H_b H - \Omega^2) \frac{d}{du} (\tilde{f} - \tilde{g})_{[x(u),y(u)]}, \end{aligned} \quad (\text{A11})$$

$$\frac{d}{du} (f + g)_{[x(u),y(u)]} = \frac{d}{du} (\tilde{f} + \tilde{g})_{[x(u),y(u)]}. \quad (\text{A12})$$

We specify $x(u) = a \cos u$; $y(u) = b \sin u$, as such parametrizing the elliptical cross section; due to the periodicity we search for solutions proportional to $\exp(inu)$ along its boundary, where n is an integer. Noting this condition and the vanishing of ψ far from the stripe, we find

$$\begin{aligned} f(Lx + iy) &= f_0 [Lx + iy + \sqrt{(Lx + iy)^2 - l^2 a^2 + b^2}]^n, \\ g(Lx - iy) &= g_0 [Lx - iy + \sqrt{(Lx - iy)^2 - l^2 a^2 + b^2}]^n, \\ \psi(x, y) &= \begin{cases} \psi_0 [x - iy + \sqrt{(x - iy)^2 - a^2 + b^2}]^n & \text{if } y > 0 \\ \psi_0 [x + iy + \sqrt{(x + iy)^2 - a^2 + b^2}]^n & \text{if } y < 0. \end{cases} \end{aligned} \quad (\text{A13})$$

Combining Eqs. (A11) and (A12), in order to eliminate ψ_0 , leads to a system of two homogeneous linear equations in f_0 and g_0 :

$$\begin{aligned} & \{ [H_b(H+4\pi M) - \Omega^2]l + 4\pi M\Omega + (H_b H - \Omega^2) \} (la + b)^n f_0 + \{ -[H_b(H+4\pi M) - \Omega^2]l + 4\pi M\Omega \\ & + (H_b H - \Omega^2) \} (la - b)^n g_0 = 0 \quad \text{for } u \in [0, \pi] \end{aligned} \quad (\text{A14})$$

and

$$\begin{aligned} & \{ [H_b(H+4\pi M) - \Omega^2]l + 4\pi M\Omega - (H_b H - \Omega^2) \} (la - b)^n f_0 \\ & + \{ -[H_b(H+4\pi M) - \Omega^2]l + 4\pi M\Omega - (H_b H - \Omega^2) \} (la + b)^n g_0 = 0 \quad \text{for } u \in [\pi, 2\pi], \end{aligned}$$

which shows nonzero solutions only for

$$\begin{aligned} & \{ (4\pi M\Omega)^2 - [(H_b(H+4\pi M) - \Omega^2)l + (H_b H - \Omega^2)]^2 \} (la + b)^{2n} \\ & = \{ (4\pi M\Omega)^2 - [- (H_b(H+4\pi M) - \Omega^2)l + (H_b H - \Omega^2)]^2 \} (la - b)^{2n}. \end{aligned} \quad (\text{A15})$$

The above described method can indeed be used in the case of an infinite plane layer of thickness $2b$: on the upper face $x(u) = u$, $y(u) = 2b$; on the lower face $x(u) = u$, $y(u) = 0$. Considering the invariance by translation in an infinite layer, we search for solutions proportional to $\exp(ixx)$. Explicitly, noting this condition and the vanishing of ψ far from the layer, we find

$$\begin{aligned}
f(lx+iy) &= f_0 \exp\left(i \frac{q}{l}(lx+iy)\right), \\
g(lx-iy) &= g_0 \exp\left(i \frac{q}{l}(lx-iy)\right), \\
\psi(x,y) &= \psi_0 \exp(iq(x+iy)) \quad \text{if } y > 2b, \\
\psi(x,y) &= \psi_0 \exp(iq(x-iy)) \quad \text{if } y < 0. \quad (\text{A16})
\end{aligned}$$

Combining Eqs. (A11) and (A12), in order to eliminate ψ_0 , leads to a system of two homogeneous linear equations in f_0 and g_0 :

$$\begin{aligned}
\{[H_b(H+4\pi M) - \Omega^2]l + 4\pi M\Omega + (H_bH - \Omega^2)\}f_0 \\
+ \{-[H_b(H+4\pi M) - \Omega^2]l + 4\pi M\Omega \\
+ (H_bH - \Omega^2)\}g_0 = 0 \quad \text{for } y=0 \quad (\text{A17})
\end{aligned}$$

and

$$\begin{aligned}
\{[H_b(H+4\pi M) - \Omega^2]l + 4\pi M\Omega - (H_bH - \Omega^2)\}f_0 \\
\times \exp\left(-\frac{2qb}{l}\right) + \{-[H_b(H+4\pi M) - \Omega^2]l + 4\pi M\Omega \\
- (H_bH - \Omega^2)\}g_0 \exp\left(\frac{2qb}{l}\right) = 0 \quad \text{for } y=2b,
\end{aligned}$$

which shows nonzero solutions only for

$$\begin{aligned}
\{(4\pi M\Omega)^2 - [(H_b(H+4\pi M) - \Omega^2)l \\
+ (H_bH - \Omega^2)]^2\} \exp\left(\frac{2qb}{l}\right) \\
= \{(4\pi M\Omega)^2 - [-(H_b(H+4\pi M) - \Omega^2)l \\
+ (H_bH - \Omega^2)]^2\} \exp\left(\frac{-2qb}{l}\right). \quad (\text{A18})
\end{aligned}$$

Now, we can compare the resulting equations for a stripe (A15) and for an infinite layer (A18). For a stripe we have

$$\left(\frac{la-b}{la+b}\right)^{2n} = \frac{(4\pi M\Omega)^2 - \{[H_b(H+4\pi M) - \Omega^2]l + (H_bH - \Omega^2)\}^2}{(4\pi M\Omega)^2 - \{-[H_b(H+4\pi M) - \Omega^2]l + (H_bH - \Omega^2)\}^2}.$$

For an infinite layer we have

$$\exp\left(-\frac{4qb}{l}\right) = \frac{(4\pi M\Omega)^2 - \{[H_b(H+4\pi M) - \Omega^2]l + (H_bH - \Omega^2)\}^2}{(4\pi M\Omega)^2 - \{-[H_b(H+4\pi M) - \Omega^2]l + (H_bH - \Omega^2)\}^2}.$$

Noticing that

$$\left(\frac{la-b}{la+b}\right)^{2n} = \left(\frac{1-b/la}{1+b/la}\right)^{2n} = \exp\left\{2n \left[\ln\left(\frac{1-b/la}{1+b/la}\right)\right]\right\} \approx \exp\left(-4n \frac{b}{la}\right),$$

we can then identify $[(la-b)/(la+b)]^{2n}$ to $\exp(-4qb/l)$ taking $q=n/a$.

*FAX: 33 (0) 1 49 40 39 38. Electronic address: cherif@lpmtm.univ-paris13.fr

¹S. Demokritov and E. Tsymbal, J. Phys. C **6**, 7145 (1994).

²B. A. Gurney, P. Baumgart, V. Speriosu, R. Fontana, A. Patlac, T. Logan, and P. Humbert (unpublished).

³B. Hillebrands, C. Mathieu, M. Bauer, S. O. Demokritov, B. Bartenlian, C. Chappert, D. Decanini, and F. Rousseaux, J. Appl. Phys. **81**, 4993 (1997).

⁴S. M. Chérif, C. Dugautier, J.-F. Hennequin, and P. Moch, J. Magn. Magn. Mater. **175**, 228 (1997).

⁵C. Mathieu, C. Hartmann, M. Bauer, O. Büttner, S. Riedling, B. Roos, S. O. Demokritov, B. Hillebrands, B. Bartenlian, C. Chappert, D. Decanini, F. Rousseaux, E. Cambriil, A. Müller, B. Hoffmann, and U. Hartmann, Appl. Phys. Lett. **70**, 2912 (1997).

⁶A. Maeda, M. Kume, T. Ogura, K. Kuroki, T. Yamada, M. Nishikawa, and Y. Harada, J. Appl. Phys. **76**, 6667 (1994).

⁷J. F. Smyth, S. Schultz, D. R. Fredkin, D. P. Kern, S. A. Rishton, H. Schmid, M. Cali, and T. R. Koehler, J. Appl. Phys. **69**, 5262 (1991).

⁸R. W. Damon and J. R. Eshbach, J. Phys. Chem. Solids **19**, 308 (1961).

⁹L. Baselgia, M. Warden, F. Waldner, S. L. Hutton, J. E. Drumheller, T. Q. He, P. E. Wigen, and M. Marysko, Phys. Rev. B **38**, 2237 (1988).

¹⁰R. Gieniusz and L. Smoczynski, J. Magn. Magn. Mater. **66**, 366 (1987).

¹¹R. E. De Wames and T. Wolfram, Prog. Surf. Sci. **2**, 233 (1972).

¹²J. F. Cochran and J. R. Dutcher, J. Appl. Phys. **63**, 3814 (1988).

¹³Y. Roussigné, F. Ganot, C. Dugautier, P. Moch, and D. Renard, Phys. Rev. B **52**, 350 (1995).

¹⁴B. Hillebrands, Phys. Rev. B **41**, 530 (1990).

¹⁵R. L. Stamps and B. Hillebrands, Phys. Rev. B **44**, 12 417 (1991).

¹⁶R. E. De Wames and T. Wolfram, Appl. Phys. Lett. **16**, 305 (1970).

¹⁷S. M. Chérif and J.-F. Hennequin, J. Magn. Magn. Mater. **165**, 504 (1997).

¹⁸R. E. Camley and L. Mills, Phys. Rev. B **26**, 2609 (1982).

¹⁹P. Beauvillain, C. Chappert, V. Grolier, R. Mégy, S. Ould-Mahfoud, J.-P. Renard, and P. Veillet, J. Magn. Magn. Mater. **121**, 503 (1993).

²⁰B. Heinrich and J. F. Cochran, Adv. Phys. **42**, 523 (1993).